ARTICLE

Surfactant-Free, Drug-Quantum-Dot Coloaded Poly(lactide-*co*-glycolide) Nanoparticles: Towards Multifunctional Nanoparticles

Barrett J. Nehilla,[†] Philip G. Allen,[‡] and Tejal A. Desai[§,*]

[†]Departments of Biomedical Engineering and Pharmacology & Experimental Therapeutics, Boston University, 44 Cummington Street, Boston, Massachusetts 02215, [‡]Department of Biomedical Engineering, Boston University, 44 Cummington Street, Boston, Massachusetts 02215, and [§]Department of Physiology and Division of Bioengineering, University of California, San Francisco, MC 2520, Byers Hall Room 203C, San Francisco, California 94158

ABSTRACT Nanoprecipitation was utilized to synthesize biodegradable and surfactant-free nanoparticles loaded with quantum dots. This protocol also yielded nanoparticles coloaded with both quantum dots and hydrophobic drug (Coenzyme Q10) molecules. Importantly, even though surfactants were not utilized during the nanoprecipitation procedure, these loaded nanoparticles did not aggregate. Dialysis efficiently removed unencapsulated quantum dots from nanoparticle suspensions without altering the physical properties of the quantum-dot-loaded nanoparticles. The resultant purified, quantum-dot-loaded nanoparticles were biocompatible in differentiated PC12 cell cultures, which facilitated their use as nanoparticles in microscopy. In fact, confocal imaging studies showed that purified, quantum-dot-loaded nanoparticles were associated with PC12 cells after one day *in vitro*. These novel and multifunctional coloaded nanoparticles may prove advantageous in future simultaneous drug delivery and imaging applications.

KEYWORDS: nanoparticles · quantum dots · Coenzyme Q10 · PLGA · confocal microscopy

Fluorescent nanocrystals, or quantum dots (QDs), have been used extensively in recent years as *in vitro* and *in vivo* imaging probes. QDs consist of a semiconductor metal core (*e.g.*, cadmium selenide) surrounded by a coating of wider bandgap semiconductor metals (*e.g.*, zinc sulfide), which significantly enhances the quantum yield of QDs.[1,2] Their unique optical properties, such as wideband excitation, narrow emission, phenomenal photostability, high quantum yield, and potential for simultaneous multicolor imaging, point to immediate advantages over conventional fluorescent dyes.[1,3] Much work has focused on QD modification for enhanced water solubility,[4] and further surface conjugation with peptides, proteins and antibodies.[5] These surface modified QDs have elicited details of receptor binding, uptake and trafficking.[5–7] Despite their numerous advantages, the semiconductor core of QDs has raised concerns of heavy metal cytotoxicity. Indeed, several studies have shown that QDs are cytotoxic by cadmium oxidation, release of heavy metal ions, and other unknown mechanisms.[8–10] As QD applications broaden in biotechnology research, it is important to consider seriously their potential hazards and develop novel approaches to avoid toxicity.

Polymeric nanoparticles are potentially interesting nanoscale materials for cell imaging and drug delivery. FDA-approved biodegradable polymers, such as the copolymer poly(lactide-*co*-glycolide) (PLGA), have been used in medical devices for many years. Protocols have been optimized for PLGA nanoparticle synthesis, and numerous drugs and small molecules have been incorporated into PLGA nanoparticles.[11] These loaded nanoparticles protect poorly soluble and unstable payloads from the biological milieu and are small enough for capillary penetration, cellular internalization, and endosomal escape.[12,13] Furthermore, their surfaces may be modified for targeted delivery of molecules to particular cells or tissues.[14] There have been few reports of fluorescent dye-loaded nanoparticles,[13,15] and these dye-loaded nanoparticles are plagued by conventional fluorescence disadvantages (*e.g.*, photobleaching). Therefore, this study explored the feasibility of combining QD advantages with those of surfactant-free PLGA nanoparticles. Specifically, QD encapsulation within surfactant-free PLGA nanoparticles *via* the nanoprecipitation protocol was investigated, and the promise of these QD-loaded nanoparticles as imaging probes was demonstrated *via* confocal microscopy. Although PLGA nano-

*Address correspondence to tejal.desai@ucsf.edu

Received for review October 5, 2007 and accepted February 01, 2008.

Published online February 13, 2008. 10.1021/nn700281b CCC: $40.75

particles are larger than QDs, they may prove advantageous as multifunctional imaging probes. Multifunctional nanoparticles incorporate various capabilities (*e.g.*, encapsulated drug release, imaging, targeting *via* conjugated ligands) in a single nanoparticle platform.[16] The potential of nanoprecipitation to yield multifunctional drug delivery and imaging nanoparticles was demonstrated by synthesizing and characterizing surfactant-free nanoparticles loaded with both a model hydrophobic drug (Coenzyme Q10, CoQ10) and QDs. The ability to track drug-loaded nanoparticles in biological systems may hasten the development of more efficacious nanoscale drug delivery systems.

RESULTS AND DISCUSSION

Empty, QD-loaded and CoQ10-QD coloaded surfactant-free PLGA nanoparticles were synthesized by the nanoprecipitation protocol. The nanoprecipitation protocol is a simple and fast technique that avoids sonication and toxic solvents.[17] Furthermore, it permits the synthesis of stabilized nanoparticles with unmodified, surfactant-free surfaces.[18] Surfactant-free surfaces are advantageous because surfactants may not be biocompatibile; they become irreversibly incorporated on nanoparticle surfaces and they alter nanoparticle surface properties.[19] Nanoprecipitation is particularly well-suited to the encapsulation of hydrophobic molecules. Therefore, it was hypothesized that hexadecylamine-capped core–shell QDs (Nanoco Technologies) could be treated as hydrophobic drug molecules and easily incorporated in PLGA nanoparticles. Although the stock QDs in toluene solubilized well in the acetone solvent, the toluene partitioned from the aqueous nonsolvent during nanoprecipitation. Therefore, the QD solvent was exchanged before nanoprecipitation by adding a small volume of QDs in toluene to 5 mL acetone (1:200, v/v). The vapor pressure of toluene was less than that of acetone but the toluene evaporated over several hours at 25 °C and acetone was supplemented back to 5 mL before nanoprecipitation. For coloaded nanoparticles, CoQ10 powder was simply dissolved in acetone before adding the QD solution. After these modifications were made, nanoprecipitation of QD- and CoQ10-QD coloaded nanoparticles was consistently achieved.

The mean diameters and polydispersity indices (PDI) of empty, QD-loaded and CoQ10-QD coloaded nanoparticles were measured by dynamic light scattering (DLS). This data demonstrated reproducible formation of surfactant-free QD- and CoQ10-QD coloaded nanoparticles with mean diameters less than 200 nm (Figure 1). The QD-loaded nanoparticles were anomalous, exhibiting significantly smaller mean diameter (153 ± 3.24 nm) and nonsignificantly higher PDI (0.143 ± 0.021) than the other samples. It was possible that trace amounts of toluene altered the solvent diffusion and solvent-polymer interactions[20] during nanoprecipitation such that smaller nanoparticles resulted. The larger diameters in CoQ10-QD coloaded nanoparticles were likely due to CoQ10 incorporation. Therefore, DLS data showed that nanoprecipitation reproducibly yielded both QD-loaded and CoQ10-QD coloaded surfactant-free nanoparticles. Phase AFM images were collected to show that these surfactant-free QD-loaded (Figure 2A) and CoQ10-QD (Figure 2B) coloaded nanoparticles were spherical and nonaggregated. Phase atomic force microscopy (AFM) images showed individual, uniformly sized QD- and CoQ10-QD-loaded nanoparticles with similar diameters as calculated by DLS. These DLS and AFM measurements strongly suggested that individual, QD- and CoQ10-QD coloaded nanoparticles could be

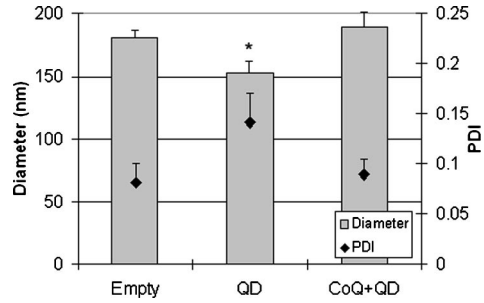

Figure 1. Diameter (grey bars) and PDI (black diamonds) of empty, QD-loaded and CoQ10-QD coloaded surfactant-free PLGA nanoparticles as measured by DLS. QD-loaded nanoparticles were significantly (*$P < 0.001$) smaller than empty and coloaded nanoparticles, although the PDI values were not statistically different ($P = 0.114$). ($n = 7$ for QD-loaded nanoparticles, $n = 5$ for others; significance determined by 1-way ANOVA with Holm-Sidak posthoc analysis).

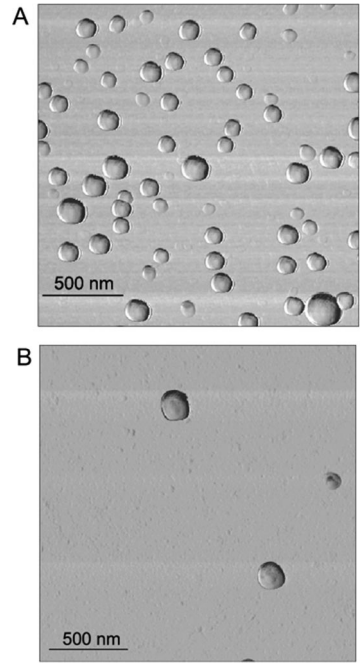

Figure 2. Representative phase AFM images of QD-loaded (A) and CoQ10-QD coloaded (B) nanoparticles showed spherical, nonaggregated morphologies and diameters that were similar to DLS measurements.

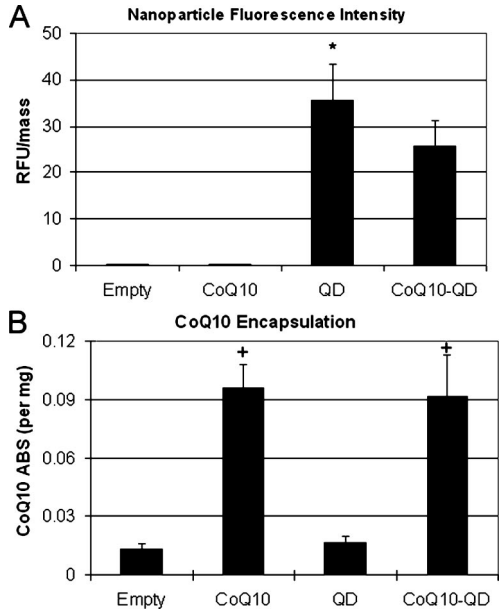

Figure 3. Encapsulation of QDs and CoQ10 within surfactant-free PLGA nanoparticles. (A) QD fluorescence in nanoparticle pellets was measured as relative fluorescence units (RFU) and then normalized to the pellet mass. QD-loaded nanoparticles were significantly (*$P = 0.002$) more fluorescent than empty and CoQ10-loaded nanoparticles, but they exhibited similar RFU/mass as the CoQ10-QD co-loaded nanoparticles. (B) CoQ10 encapsulation was determined spectrophotometrically and then normalized to nanoparticle mass. CoQ10-loaded and CoQ10-QD coloaded nanoparticles exhibited significantly higher ($^{+}P = 0.002$) CoQ10 absorbance values than empty and QD-loaded nanoparticles. ($n = 5$ for QD fluorescence, $n = 4$ for CoQ10 absorbance; significance determined by 1-way ANOVA with Dunn's posthoc analysis).

easily synthesized *via* nanoprecipitation without the presence of surfactants.

The next step was to confirm QD and CoQ10 encapsulation within the nanoparticles. After nanoprecipitation, QD-loaded and CoQ10-QD coloaded nanoparticle suspensions were centrifuged. Preliminary work showed that unencapsulated QDs, unencapsulated CoQ10, and free PLGA were removed by aspirating the supernatant because these unencapsulated molecules did not pellet with the loaded nanoparticles. QD encapsulation within PLGA nanoparticles was determined by measuring the fluorescence intensity of the resuspended pellets (Figure 3A). The QD-loaded nanoparticles were significantly more fluorescent than empty nanoparticles. Additionally, the CoQ10-QD coloaded nanoparticles were significantly more fluorescent than both empty and CoQ10-loaded nanoparticles. These fluorescence measurements showed that QDs were successfully encapsulated in PLGA nanoparticles *via* nanoprecipitation. Furthermore, the presence of CoQ10 did not alter QD encapsulation in the coloaded nanoparticles. Next, CoQ10 encapsulation in the coloaded nanoparticles was confirmed by lyophilizing the nanoparticles and spectrophotometrically measuring CoQ10 absorbance (Figure 3B). Very little CoQ10 was detected in empty or QD-loaded nanoparticles but CoQ10 encapsulation in CoQ10-QD coloaded nanoparticles closely matched that of CoQ10-loaded nanoparticles. Therefore, CoQ10 was successfully incorporated in the co-loaded nanoparticles. Taken together, QD fluorescence and CoQ10 absorbance measurements clearly demonstrated CoQ10 and QD coencapsulation in the same nanoparticle. This is the first known demonstration of coloading of QDs and any other molecule within surfactant-free biodegradable nanoparticles. Therefore, both QD-loaded and CoQ10-QD coloaded surfactant-free PLGA nanoparticles are feasible *via* nanoprecipitation.

In other recent work, QDs were encapsulated within poly(D,L-lactide) nanoparticles *via* nanoprecipitation.[10,21] A major disadvantage of those QD-loaded nanoparticles was that surfactants were utilized during nanoprecipitation. Our surfactant-free nanoparticles are advantageous because surfactants are irremovable from nanoparticle surfaces, they alter nanoparticle biocompatibility, they alter surface properties, and they may block access to easily modified surface carboxyl groups.[19] Therefore, the current QD-loaded, surfactant-free biodegradable nanoparticles were a significant technological improvement. The CoQ10-QD coloaded nanoparticles also demonstrated nanoprecipitation's versatility. Researchers familiar with nanoprecipitation can easily incorporate QDs into already characterized drug-loaded nanoparticles without laborious alterations in the protocol, thus forming multifunctional drug-QD coloaded nanoparticles for simultaneous drug delivery and imaging.

Separating unencapsulated QDs from QD-loaded nanoparticles was essential for successful imaging and biocompatibility experiments. Since QD encapsulation was not 100% efficient, unencapsulated QDs were present in the nanoparticle suspension after nanoprecipitation. These unencapsulated QDs could cause cytotoxicity since they were not encapsulated within PLGA nanoparticles, and they could complicate microscopy image analysis. For example, the $x-y$ resolution of light microscopy modalities was not sufficient to resolve unencapsulated QDs from small clusters of QDs within larger PLGA nanoparticles; individual QD resolution is only realistic with AFM or electron microscopy. Therefore, a nondestructive purification protocol was needed to separate unencapsulated QDs from QD-loaded nanoparticles. Unfortunately, QD-loaded nanoparticles could not be resuspended into individual particles after centrifugation because of their surfactant-free surfaces.[18] However, unencapsulated QDs traversed high-molecular-weight cutoff (50 kDa) dialysis tubing. Therefore, the QD-loaded nanoparticle suspension was dialyzed immediately after nanoprecipitation, which removed unencapsulated QDs and yielded purified, surfactant-free, QD-loaded nanoparticles.

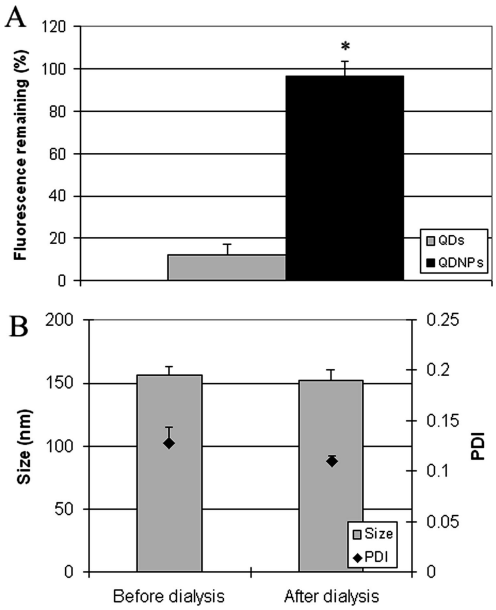

Figure 4. QD-loaded nanoparticle purification by dialysis was successful and nondestructive. (A) After 1 day of dialysis, QD-loaded nanoparticle suspensions (black) contained significantly (*$P < 0.001$) more QD fluorescence than free QD suspensions (grey), which suggested that unencapsulated QDs traversed the dialysis membrane. (B) The diameter ($P = 0.801$) and PDI ($P = 0.335$) of QD-loaded nanoparticles before and after purification were statistically the same, which showed that purification was nondestructive. ($n = 9$; significance determined by *t* tests).

Successful removal of unencapsulated QDs by dialysis was confirmed by fluorescence measurements. A solution of free QDs, prepared exactly as for QD-loaded nanoparticles, but without PLGA, was used as the control. After one day of dialysis, the fluorescence of free QD suspensions was 12 ± 4.7% of undialyzed QD suspensions. By contrast, QD-loaded nanoparticle suspensions retained 97 ± 7.3% of the undialyzed fluorescence (Figure 4A). These data indicated that the unencapsulated QDs were small enough to cross the dialysis membrane, but the QD-loaded nanoparticles remained inside the tubing. In fact, the dialysis membrane pore diameters were roughly 3–3.5 nm (personal communication with Membrane Filtration Products, Inc.), which is approximately the same size as free QDs. Additionally, nonspecific binding of free QDs to the dialysis membrane likely contributed to the loss of fluorescence. On the other hand, the QD-loaded nanoparticle suspension retained fluorescence during dialysis because many QDs were incorporated during nanoprecipitation. The physical properties of the purified QD-loaded nanoparticles were then analyzed (Figure 4B) to confirm the physically nondestructive nature of this dialysis purification protocol. The diameter and PDI of purified, QD-loaded nanoparticles (153 ± 6.99 and 0.109 ± 0.005 nm, respectively) were both lower, but not significantly different from unpurified QD-loaded nanoparticles (156 ± 7.15 and 0.128 ± 0.016 nm). The PDI likely decreased because of the loss of unencapsulated QDs.

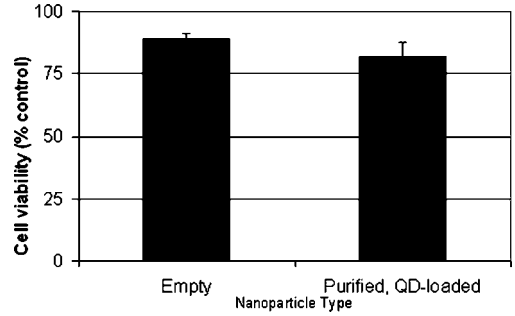

Figure 5. Empty and purified, QD-loaded nanoparticles were not acutely cytotoxic to differentiated PC12 cells. The cytotoxicity was measured by the MTT assay and normalized to DIH_2O-treated controls. After 3 days of treatment, purified QD-loaded nanoparticles were no more cytotoxic ($P = 0.238$) than empty nanoparticles. ($n = 3$; significance determined by *t* test).

These results showed that individual, surfactant-free QD-loaded nanoparticles were stable and unmodified during the simple dialysis procedure that purified QD-loaded nanoparticles of unencapsulated QDs.

It was important to investigate the acute cytotoxicity of QD-loaded nanoparticles before applying them to cells for drug delivery or imaging studies. Differentiated PC12 cells were chosen because they are well-characterized as models to study neurotrophin action, neuronal differentiation, protein trafficking, and vesicle dynamics.[22] Furthermore, protein-conjugated QDs have been used as imaging nanoparticles in differentiated PC12 cells.[7] These preliminary cytotoxicity experiments were important because surfactant-free nanoparticle cytotoxicity has not been investigated *in vitro*[23,24] and because there were no known reports of PLGA nanoparticle biocompatibility with PC12 cells. Furthermore, QDs have caused oxidative stress-mediated cytotoxicity *via* semiconductor metal oxidation, although toxicity is cell-type and surface-coating dependent.[8–10,21,25] Laborious surface modification of QD core/shell structures with various polymers and biomolecules has been utilized to form a barrier to metal ion diffusion.[9] It was hypothesized that by incorporating QDs into the core of larger PLGA nanoparticles, both the oxidation-induced metal catalysis and the release of toxic metal ions would be significantly diminished.

Empty and purified, QD-loaded nanoparticles were exposed to 254 nm ultraviolet light to oxidize the QD cadmium core. They were then applied to differentiated PC12 cells. After 3 days of exposure, cytotoxicity was assessed with the MTT assay (Figure 5). The viability of cells exposed to 33 μg/mL QD-loaded nanoparticles (82 ± 6.2% of control) was not significantly lower than the viability of cells exposed to 100 μg/mL empty nanoparticles (89 ± 2.0% of control). The disparity in nanoparticle concentration was due to QD-loaded nanoparticle loss during dialysis. In other work, a wide range of upper limits for PLGA nanoparticle biocompatibility has been reported, from as low as 80 μg/mL to hundreds of μg/mL.[15,26,27] However, comparing the current data

to published work was difficult because of the lack of cell studies with QD-loaded nanoparticles and the different measurements of QD concentrations. Up to 100 μg/mL of QD-loaded chitosan nanoparticles were not toxic after one day,[25] but surface modified, QD-loaded PLA nanoparticles completely killed cells at concentrations as low as 100 ppm after two days.[21] Many PLGA nanoparticle characteristics contribute to their overall biocompatibility, especially their surface characteristics, and their toxicity is cell-line dependent. Furthermore, although very little QD release from the nanoparticles is expected over three days because of QD hydrophobicity,[18] it is possible that a small concentration of individual QDs contributed to the cytotoxicity of the QD-loaded nanoparticles. Given the general paucity of surfactant-free nanoparticle toxicity data and the specific lack of nanoparticle biocompatibility data in the PC12 cell line, it was important to establish the cytotoxicity of purified, QD-loaded nanoparticles. Because these surfactant-free QD-loaded nanoparticles were biocompatible with differentiated PC12 cells, short-term imaging studies were performed without concern for nanoparticle-induced acute toxicity.

After purifying QD-loaded nanoparticles, confocal microscopy was used to investigate nanoparticle−cell interactions. Since the release of extremely hydrophobic compounds like CoQ10 is on the order of days,[18] QD release from surfactant-free nanoparticles is likely on a similar time scale. Therefore, very few individual QDs were expected in the confocal imaging studies after one day. Furthermore, the purified formulation of QD-loaded nanoparticles provided assurance that red fluorescence originated from QD-loaded nanoparticles but not unencapsulated QDs. Differentiated PC12 cells were exposed to 33 μg/mL purified, QD-loaded nanoparticles for one day and then stained, fixed, and analyzed at 40× magnification. Some red QD-loaded nanoparticles were associated with green differentiated PC12 cells (Figure 6), but *z*-stack movies showed that many QD-loaded nanoparticles settled on the glass imaging surface. To visualize the 3-dimensional localization of selected QD-loaded nanoparticles, the images were resliced (Figure 6: 1, 2, 3) so that the resliced *y*-axis represented the original *z*-axis. The resliced images (Figure 6: 1, 2, 3) effectively represent the *z*-stack of images at the linear regions specified in Figure 6. These representative slices showed punctate red fluorescence at the fringes of, but not surrounded by, green PC12 cell fluorescence. Furthermore, there is no yellow overlap of red and green fluorescence. On the basis of this analysis, QD-loaded nanoparticles interacted with differentiated PC12 cell surfaces, but endocytosis could not be established. This confocal analysis (and thus single nanoparticle detection) was limited by both the *z* resolution of 1.19 μm/slice and the *x*−*y* resolution of 0.206 μm/pixel. Therefore, individual QD-loaded nanoparticles could not be localized to volumes smaller than that

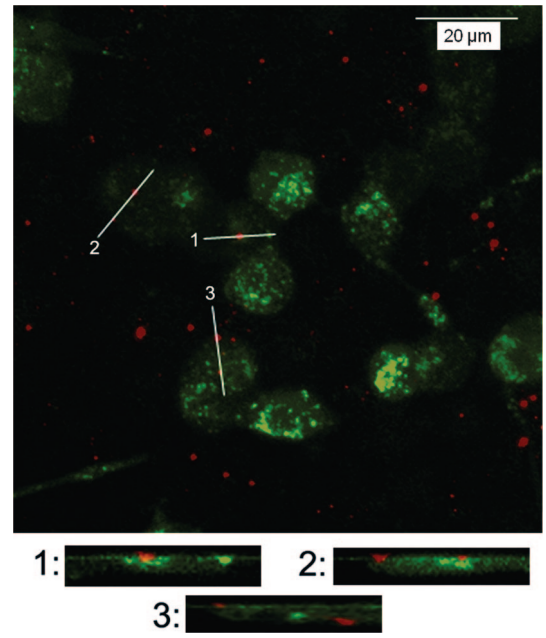

Figure 6. Confocal microscopy image (40×) of differentiated PC12 cells (green) and purified, QD-loaded nanoparticles (red) with three resliced regions of interest (labeled 1, 2, 3). Much red fluorescence was localized on the glass imaging surface, but regions with PC12 cell-associated QD-loaded nanoparticles were resliced using ImageJ. The resliced images (1, 2, 3) showed that QD-loaded nanoparticles were associated with cell surfaces at the fringes of green fluorescence, but their internalization could not be definitively determined with this analysis.

dictated by the *x*, *y*, and *z* resolutions. Since red fluorescence was present in several *z*-slices in the resliced images (1, 2, and 3 in Figure 6), it was possible that QD-loaded nanoparticles were internalized but localized near the inner plasma membrane surface. This possibility, in addition to nanoparticle surface modification for enhanced internalization, warrants investigation in future work. QD-loaded nanoparticle internalization was expected because of previous reports of nanoparticle endocytosis,[13] particularly *via* tyrosine kinase A receptors in differentiated PC12 cells.[7] In that study, the modified QDs were much smaller than the current QD-loaded nanoparticles. Since nanoparticle internalization by cells is highly size-dependent,[28] much lower levels of QD-loaded nanoparticle endocytosis (compared to protein-modified QDs) were admissable. In the future, PLGA carboxyl groups may be modified for surface conjugation of targeting ligands, which may enhance the endocytosis and intracellular delivery of these QD-loaded nanoparticles.

This study showed that nanoprecipitation is a versatile protocol for synthesizing novel, surfactant-free fluorescent polymeric nanoparticles. QDs were successfully encapsulated within PLGA nanoparticles, and these QD-loaded nanoparticles were easily purified of potentially toxic unencapsulated QDs by dialysis. Simply dissolving the model hydrophobic drug CoQ10 in the solvent before nanoprecipitation

yielded CoQ10-QD coloaded nanoparticles, which hold promise for simultaneous drug delivery and imaging applications. The purified QD-loaded nanoparticles were biocompatible at the concentrations applied for confocal imaging applications, and these nanoparticles were associated with differentiated PC12 cells after one day. The novelty, simplicity of synthesis, and similarity to other PLGA nanoparticles are major advantages of these QD-loaded and CoQ10-QD coloaded nanoparticles.

EXPERIMENTAL METHODS

Synthesis of QD-Loaded and CoQ10-QD Coloaded Nanoparticles. Nanoparticles were synthesized by the nanoprecipitation protocol.[17,18] A stock solution of hexadecylamine-capped cadmium selenide−zinc sulfide core–shell QDs with 610 ± 10 nm emission (Nanoco, Manchester, U.K.) was prepared in toluene at 5 mg/mL and stored at −20 °C. For synthesis, 25 μL QD solution was added to 5 mL of 10 mg/mL carboxylic acid-terminated PLGA (0.67 dL/g, Lactel Absorbable Polymers, Pelham, Alabama) in acetone, and the toluene was evaporated for several hours at 25 °C. For coloaded nanoparticles, the 10 mg/mL PLGA solution also contained 400 μg/mL CoQ10. The QD and PLGA solution was brought to 5 mL and sonicated briefly before injection into 100 mL of stirred DIH_20. After overnight magnetic spinning for acetone evaporation to air, the nanoparticle suspension was qualitatively filtered (Whatman 1) and subjected to further experimentation.

Physical Characterization of Nanoparticles. For nanoparticle size and polydispersity index (PDI) analyses, dynamic light scattering (DLS) was performed at room temperature with a scattering angle of 90° (90Plus Particle Size Analyzer, Brookhaven Instruments Corp., Holtsville, NY). DLS calculates diameters and PDIs from the fluctuations of scattered light intensities due to the Brownian motion of nanoparticles in suspension. Each measurement was the average of five 1-min runs. For morphology analysis, silicon chips were first cleaned and hydrophilized in Piranha solution for 30 min, followed by vigorous washing in DIH_2O. Piranha solution consisted of 3:1 97% sulfuric acid/30% hydrogen peroxide and was freshly prepared before use. Silicon chips were then silanized in 2% (v/v) 3-aminopropyltriethoxysilane in acetone for 30 min and briefly rinsed with acetone. Then, 5 μL of nanoparticle suspension was adsorbed on silanized silicon chips for 20 min before delicate rinsing with DIH_2O and drying under a nitrogen stream. The nanoparticles were then scanned by tapping mode atomic force microscopy (AFM) operated in phase imaging mode (Quesant Q-250, Ambios Technology).

Determination of Quantum Dot Incorporation. To measure QD incorporation within nanoparticles, free PLGA, QDs and/or CoQ10 were separated from the nanoparticles by centrifugation at 17200*g* for 30 min at 25 °C. After washing the nanoparticle pellet three times in 30 mL of DIH_2O to remove unencapsulated QDs, nanoparticles were resuspended in 2 mL of DIH_2O. The fluorescence (300 nm excitation/630 nm emission wavelengths) of 0.3 mL of this suspension was measured on a microplate fluorimeter (SpectraMax M5, Molecular Devices, Sunnyvale, CA) in relative fluorescence units (RFU). The remainder of this solution was then frozen, lyophilized, and analyzed for CoQ10 encapsulation, as described below.

Determination of CoQ10 Incorporation. To measure CoQ10 encapsulation, free PLGA, QDs, and/or CoQ10 were separated from the nanoparticles by centrifugation (RC-5C Plus, Sorvall, Asheville, NC) at 17200*g* for 30 min at 25 °C. The nanoparticle pellet was washed three times with 30 mL of DIH_2O, resuspended in 2 mL of DIH_2O and frozen at −80 °C. After freezing, the nanoparticles were lyophilized for two days (Virtis Benchtop SLC, Gardiner, NY). The lyophilized nanoparticle mass was measured before dissolving the nanoparticles in acetonitrile. CoQ10 encapsulation was determined spectrophotometrically at 275 nm and then normalized to the nanoparticle mass.

Purification of QD-Loaded Nanoparticles. QD-loaded nanoparticles were separated from unencapsulated QDs by dialysis. Immediately after solvent evaporation, unpurified suspensions of QD-loaded nanoparticles and free QDs were loaded into 50 kDa MWCO dialysis tubing (Membrane Filtration Products, Seguin, TX). The free QD suspension was prepared exactly as for QD-loaded nanoparticles, but in the absence of PLGA. Dialysis was performed against DIH_2O for 24 h at 25 °C with several buffer changes. After dialysis, the purified suspensions were qualitatively filtered (Whatman 1) and analyzed for fluorescence intensity, as described above. For each sample, a control solution of undialyzed QDs or QD-loaded nanoparticles was measured for fluorescence along with the dialyzed sample. The percent decrease in fluorescence was quantified for free QDs and QD-loaded nanoparticles.

Cells. The PC12 pheochromocytoma cell line (ATCC, Manassas, VA) was utilized for cell labeling experiments. Cells were routinely maintained at 37 °C in 5% CO_2 in RPMI-1640 media supplemented with 10% horse serum and 5% fetal bovine serum (sera from ATCC). For microscopy, poly D-lysine coated glass bottom cell culture dishes (Mattek, Ashland, MA) were overcoated with 50 μg/mL collagen I from rat tail (BD Biosciences, San Jose, CA) before cell seeding. For cytotoxicity assays, 12-well plates (Corning) were coated with 50 μg/mL collagen I before cell seeding. After cells attached to the substrates, media was replaced with complete RPMI-1640 supplemented with 25 ng/mL 2.5S nerve growth factor (NGF; BD Biosciences). The PC12 cells differentiated in the presence of NGF for 3 days before experiments were conducted.

Cytotoxicity Assay. Empty and purified, QD-Loaded nanoparticles were exposed to UV light (254 nm) for 48 h to oxidize the QD core and promote cadmium ion leakage. In the meantime, PC12 cells were plated in collagen-coated 12-well plates at an approximate density of 3500 cells/cm^2. After attachment, cells were treated with 25 ng/mL NGF for 3 days before applying the nanoparticles. One mL of the nanoparticle samples were applied to each well with 2 mL of NGF-supplemented media incubated for 3 days. To perform the MTT assay, media was removed and replaced with 0.5 mL RPMI without phenol red. MTT solution (5 mg/mL) was added to each well (10% total well volume) and allowed to react for 3 h at 37 °C. MTT formazan crystals were then dissolved in MTT solvent. Values were determined by subtracting 690 from 570 nm absorbance, and then normalized to sterile DIH_2O-treated controls.

Microscopy. Laser-scanning confocal fluorescent microscopy was performed to visualize interactions of the QD-loaded nanoparticles with differentiated PC12 cells. After one day of treatment with 1 mL of purified QD-loaded nanoparticles, the cells were stained with 5 μM 5-chloromethylfluorescein (CMFDA; Invitrogen, Carlsbad CA). The dye was taken up during 30 min of incubation at 37 °C, and then the dye-containing media was replaced with complete RPMI. The cells were then incubated for another 30 min at 37 °C. Afterward, cells were fixed in 3% paraformaldehyde for 20 min at 25 °C and visualized in complete RPMI without phenol red.

An Olympus IX81 microscope with the Fluoview 1000 confocal scanning microscopy (FV10-ASW, Melville, NY) setup was used. The sample was excited with a 405 nm diode laser for QD emission at 610 nm and the 488 nm argon laser line for CMFDA emission at 515 nm. Images were acquired at 40× with a sampling speed of 8 μs/pixel and the optimal *z*-step size of 1.19 μm/slice. The 40 pixel × 512 pixel × 512 pixel images were 105.472 μm^2 (0.206 μm/pixel).

All postacquisition image processing was performed with ImageJ software (v1.33u). To investigate the cellular interactions of individual QD-loaded nanoparticles, importing images without compromising light intensity data was critical. For *z*-stacked color images, each channel of 16-bit confocal images was imported as a sequence (30 slices for 40× images) and then converted to RGB images. Afterward, the images were merged, pixel size was set to "no scale", and the images were analyzed. A lin-

ear region of interest (ROI) within these stacked images was selected to include a QD-loaded nanoparticle and a PC12 cell. These ROIs were resliced to yield a cross section. Thus, the *y*-axis of the resliced image represents the original *z*-axis at the selected ROI. Before converting the images to CMYK format for presentation, the green channel of the resliced images was enhanced in Adobe Photoshop (v6.0.1) by decreasing the input level from 255 to 100. The enhanced green channel in these cross section images permitted easier visualization of red QD-loaded nanoparticle localization with respect to green fluorescent cells.

Acknowledgements The authors thank the American Foundation for Aging Research (AFAR) for partial financial support of this work and NIH (NEI).

REFERENCES AND NOTES

1. Chan, W. C.; Nie, S. Quantum dot Bioconjugates for Ultrasensitive Nonisotopic Detection. *Science* **1998**, *281*, 2016–2018.
2. Dabbousi, B.; Rodriguez-Viejo, J.; Mikulec, F. V.; Heine, J. R.; Mattoussi, H.; Ober, R.; Jensen, K. F.; Bawendi, M. G. (CdSe)ZnS Core-Shell Quantum Dots: Synthesis and Characterization of a Size Series of Highly Luminescent Nanocrystallites. *J. Phys. Chem. B* **1997**, *101*, 9463–9475.
3. Jaiswal, J. K.; Simon, S. M. Potentials and Pitfalls of Fluorescent Quantum Dots for Biological Imaging. *Trends Cell Biol.* **2004**, *14*, 497–504.
4. Bruchez, M., Jr.; Moronne, M.; Gin, P.; Weiss, S.; Alivisatos, A. P. Semiconductor Nanocrystals as Fluorescent Biological Labels. *Science* **1998**, *281*, 2013–2016.
5. Gao, X.; Cui, Y.; Levenson, R. M.; Chung, L. W. K.; Nie, S. *In Vivo* Cancer Targeting and Imaging with Semiconductor Quantum Dots. *Nat. Biotechnol.* **2004**, *22*, 969–976.
6. Jaiswal, J. K.; Mattoussi, H.; Mauro, J. M.; Simon, S. M. Long-term Multiple Color Imaging of Live Cells Using Quantum Dot Bioconjugates. *Nat. Biotechnol.* **2003**, *21*, 47–51.
7. Sundara Rajan, S.; Vu, T. Q. Quantum Dots Monitor TrkA Receptor Dynamics in the Interior of Neural PC12 Cells. *Nano Lett.* **2006**, *6*, 2049–2059.
8. Derfus, A. M.; Chan, W. C. W.; Bhatia, S. N. Probing the Cytotoxicity of Semiconductor Quantum Dots. *Nano Lett.* **2004**, *4*, 11–18.
9. Hardman, R. A Toxicological Review of Quantum Dots: Toxicity Depends on Physicochemical and Environmental Factors. *Environ. Health Perspect.* **2006**, *114*, 165–72.
10. Guo, G.; Liu, W.; Liang, J.; Le, Z.; Xu, H.; Yang, X. Preparation and Characterization of Novel CdSe Quantum Dots Modified with Poly(D,L-lactide) Nanoparticles. *Mater. Lett.* **2006**, *60*, 2565–2568.
11. Hans, M. L.; Lowman, A. M. Biodegradable Nanoparticles for Drug Delivery and Targeting. *Curr. Opin. Solid State Mater. Sci.* **2002**, *6*, 319–327.
12. Soppimath, K. S.; Aminabhavi, T. M.; Kulkarni, A. R.; Rudzinski, W. E. Biodegradable Polymeric Nanoparticles as Drug Delivery Devices. *J. Controlled Release* **2001**, *70*, 1–20.
13. Panyam, J.; Zhou, W. Z.; Prabha, S.; Sahoo, S. K.; Labhasetwar, V. Rapid Endo-Lysosomal Escape of Poly(D,L-lactide-*co*-glycolide) Nanoparticles: Implications for Drug and Gene Delivery. *FASEB J.* **2002**, *16*, 1217–1226.
14. Nobs, L.; Buchegger, F.; Gurny, R.; Allémann, E. Poly(lactic acid) Nanoparticles Labeled with Biologically Active Neutravidin™ for Active Targeting. *Eur. J. Pharm. Biopharm.* **2004**, *58*, 483–90.
15. Davda, J.; Labhasetwar, V. Characterization of Nanoparticle Uptake by Endothelial Cells. *Int. J. Pharm.* **2002**, *233*, 51–9.
16. Torchilin, V. P. Multifunctional Nanocarriers. *Adv. Drug Delivery Rev.* **2006**, *58*, 1532–55.
17. Fessi, H.; Puisieux, F.; Devissaguet, J. P.; Ammoury, N.; Benita, S. Nanocapsule Formation by Interfacial Polymer Deposition Following Solvent Displacement. *Int. J. Pharm.* **1989**, *55*, R1–R4.
18. Nehilla, B. J.; Bergkvist, M. B.; Popat, K. C.; Desai, T. A. Purified and Surfactant-free Coenzyme Q10-Loaded Biodegradable Nanoparticles. *Int. J. Pharm.* **2008**, *348*, 107–114.
19. Sahoo, S. K.; Panyam, J.; Prabha, S.; Labhasetwar, V. Residual Polyvinyl Alcohol Associated with Poly (D,L-lactide-*co*-glycolide) Nanoparticles Affects their Physical Properties and Cellular Uptake. *J. Controlled Release* **2002**, *82*, 105–14.
20. Choi, S.-W.; Kwong, H. Y.; Kim, W. S.; Kim, J. H. Thermodynamic Parameters on Poly(D,L-lactide-*co*-glycolide) Particle Size in Emulsification-Diffusion Process. *Colloids Surf., A* **2002**, *201*, 283–289.
21. Guo, G.; Liu, W.; Liang, J.; Le, Z.; Xu, H.; Yang, X. Probing the Cytotoxicity of CdSe Quantum Dots with Surface Modification. *Mater. Lett.* **2007**, *61*, 1641–1644.
22. Greene, L. A.; Tischler, A. S. Establishment of a Noradrenergic Clonal Line of Rat Adrenal Pheochromocytoma Cells which Respond to Nerve Growth Factor. *Proc. Natl. Acad. Sci. U.S.A.* **1976**, *73*, 2424–8.
23. Jeong, Y.-I.; Shim, Y.-H.; Kim, C; Lim, G.-T.; Choi, K.-C.; Yoon, C. Effect of Cryoprotectants on the Reconstitution of Surfactant-Free Nanoparticles of Poly(D,L-lactide-*co*-glycolide). *J. Microencapsulation* **2005**, *22*, 293–601.
24. Lamalle-Bernard, D.; Munier, S.; Compagnon, C.; Charles, M.-H.; Kalyanaraman, V. S.; Delair, T.; Verrier, B.; Önal, Y. A. Coadsorption of HIV-1 p24 and gp120 Proteins to Surfactant-free Anionic PLA Nanoparticles Preserves Antigenicity and Immunogenicity. *J. Controlled Release* **2006**, *115*, 57–67.
25. Tan, W. B.; Huang, N; Zhang, Y. Ultrafine Biocompatible Chitosan Nanoparticles Encapsulating Multi-Coloured Quantum Dots for Bioapplications. *J. Colloid Interface Sci.* **2007**, *310*, 464–470.
26. Cegnar, M.; Premzl, A.; Zavasnik-Bergant, V.; Kristl, J.; Kos, J. Poly(lactide-*co*-glycolide) Nanoparticles as a Carrier System for Delivering Cysteine Protease Inhibitor Cystatin into Tumor Cells. *Exp. Cell Res.* **2004**, *301*, 223–31.
27. Westedt, U.; Kalinowski, M.; Wittmar, M.; Merdan, T.; Unger, F.; Fuchs, J.; Schäller, S.; Bakowsky, U.; Kissel, T. Poly(vinyl alcohol)-graft-poly(lactide-*co*-glycolide) Nanoparticles for Local Delivery of Paclitaxel for Restenosis Treatment. *J. Controlled Release* **2007**, *119*, 41–51.
28. Desai, M. P.; Labhasetwar, V.; Walter, E.; Levy, R. J.; Amidon, G. L. The Mechanism of Uptake of Biodegradable Microparticles in Caco-2 Cells Is Size Dependent. *Pharm. Res.* **1997**, *14*, 1568–73.